The Journal of Neuroscience, March 1, 2002, 22(5):1550–1561

Consequences of the Stoichiometry of *Slo1* α and Auxiliary β Subunits on Functional Properties of Large-Conductance Ca^{2+}-Activated K^+ Channels

Ying-Wei Wang, Jiu Ping Ding, Xiao-Ming Xia, and Christopher J. Lingle

Departments of Anesthesiology and Anatomy and Neurobiology, Washington University School of Medicine, St. Louis, Missouri 63110

Auxiliary β subunits play a major role in defining the functional properties of large-conductance, Ca^{2+}-dependent BK-type K^+ channels. In particular, both the β1 and β2 subunits produce strong shifts in the voltage dependence of channel activation at a given Ca^{2+}. β subunits are thought to coassemble with α subunits in a 1:1 stoichiometry, such that a full ion channel complex may contain up to four β subunits per channel. However, previous results raise the possibility that ion channels with less than a full complement of β subunits may also occur. The functional consequence of channels with differing stoichiometries remains unknown. Here, using expression of α and β subunits in *Xenopus* oocytes, we show explicitly that functional BK channels can arise with less than four β subunits. Furthermore, the results show that, for both the β1 and β2 subunits, each individual β subunit produces an essentially identical, incremental effect on the voltage dependence of gating. For channels arising from α + β2 subunits, the number of β2 subunits per channel also has a substantial impact on properties of steady-state inactivation and recovery from inactivation. Thus, the stoichiometry of α:β subunit assembly can play a major functional role in defining the apparent Ca^{2+} dependence of activation of BK channels and in influencing the availability of BK channels for activation.

Key words: auxiliary subunits; BK channels; Ca^{2+}- and voltage-gated K^+ channels; Slo1 *channels; inactivation; ion channel stoichiometry; gating mechanisms*

Large-conductance, Ca^{2+}-activated BK-type K^+ channels exhibit substantial functional diversity (McManus, 1991; Vergara et al., 1998) contributed, in part, from coexpression of the pore-forming *Slo* α subunit (Adelman et al., 1992; Butler et al., 1993) with members of an auxiliary β subunit family. At present, four mammalian β subunits have been identified (Knaus et al., 1994b; Wallner et al., 1999; Xia et al., 1999, 2000; Brenner et al., 2000; Meera et al., 2000; Uebele et al., 2000; Weiger et al., 2000). Both the β1 and β2 subunits result in pronounced negative shifts in the voltage of half-activation at a given $[Ca^{2+}]$ (McManus et al., 1995; Wallner et al., 1995, 1999; Xia et al., 1999; Brenner et al., 2000). Both the β2 (Wallner et al., 1999; Xia et al., 1999) and β3b (Uebele et al., 2000; Xia et al., 2000) subunits result in kinetically distinct inactivating BK channels.

β subunits can exist in a 1:1 stoichiometry with α subunits (Knaus et al., 1994a): four β subunits can coassemble with four α subunits into an intact BK channel. Previous work on inactivating BK (BK_i) channels in rat chromaffin cells (Ding et al., 1998) suggests that the variability in inactivation behavior might arise from differential stoichiometry of some inactivation-competent subunit in the channel population (Ding et al., 1998). Given the presence of β2 subunit message in rat chromaffin cells (Xia et al., 1999) and the similarity of α + β2 currents to BK_i currents (Wallner et al., 1999; Xia et al., 1999), one possibility is that, in rat chromaffin cells, channels occur with less than a 1:1 assembly of β2:α subunits. The dependence of BK channel properties on β:α coassembly was also examined in *Xenopus* oocytes by varying the ratio of coinjected β1 and α subunits (Jones et al., 1999). This work proposed the view that β1 subunits produced an all-or-none shift in gating properties of the resulting BK channels (Jones et al., 1999).

These previous studies raise interesting questions concerning the functional consequences that result from less than a full 1:1 stoichiometric assembly of β and α subunits BK. First, it remains unclear whether BK channels can form with less than four β subunits. Second, if BK channels can contain less than four β subunits, what is the role that a single β subunit plays in influencing the various functional properties of the channel? To address these issues, we use the inactivation properties conferred on BK channels by the β2 subunit as an indicator of β2:α subunit stoichiometry within a channel population that can then be related to other functional properties. The results demonstrate that BK channels that contain less than four β subunits can occur. Furthermore, channels with less than a full complement of β subunits show gating properties and inactivation behavior that scale with the average number of β subunits per channel.

MATERIALS AND METHODS

Expression in Xenopus *oocytes.* The preparation of the β1 and β2 expression constructs used here has been described previously (Xia et al., 1999). Two other constructs used here were also described in previous work (Xia et al., 1999): first, the β2-Δ33 construct in which 33 N-terminal amino acids were removed from the β2 subunit; and second, a construct in which the 33 initial amino acids from the β2 N terminus were appended to the N terminus of the β1 subunit. This latter construct is here termed β1–C2. The α subunit used here was the mouse *Slo1* construct used previously (Xia et al., 1999), which corresponds to a zero amino acid insert at splice site 1 and a three amino acid insert at splice

Received Nov. 2, 2001; revised Dec. 7, 2001; accepted Dec. 7, 2001.

This work was supported by National Institutes of Health Grants DK46564 and NS37671. We thank Lynn Lavack for injection and care of oocytes.

Correspondence should be addressed to Chris Lingle, Department of Anesthesiology, Washington University School of Medicine, Box 8054, St. Louis, MO 63110. E-mail: clingle@morpheus.wustl.edu.

site 2. Methods of expression in *Xenopus* oocytes were as described previously (Xia et al., 1999).

After injection, oocytes were maintained in ND96 (in mM: 96 NaCl, 2.0 KCl, 1.8 $CaCl_2$, 1.0 $MgCl_2$, and 5.0 HEPES, pH 7.5) supplemented with sodium pyruvate (2.5 mM), penicillin (100 U/ml), streptomycin (100 mg/ml), and gentamycin (50 mg/ml). Oocytes were used for electrophysiological experiments 1–7 d after injection of cRNA.

Ratios of the injected β:α subunits are identified in specific experiments. These ratios reflect the ratio of weights of injected material. cRNA preparations typically result in ~1 ng/μl, regardless of RNA species. The molecular weight of *Slo1* α cRNA is approximately fivefold greater than that of β1 and β2 cRNA. Thus, at a 1:1 ratio by weight, β subunits are expected to be in an approximately fivefold molar excess over α subunits. In our experience, the same nominally identical ratio may not yield identical results over time or in different batches of oocytes, even when we are reasonably confident that RNA degradation has been minimized. To minimize degradation problems that might be associated with freezing and thawing, each preparation of RNA was separated into aliquots at the time of preparation, and a separate aliquot was used for each injection. Another potential problem is that, for distinct nonhomologous RNA species (i.e., α and β cRNA), it is not clear how the injected ratio may relate to the stoichiometry of assembly. To circumvent this problem, we have therefore used the properties of inactivation as independent estimators of the stoichiometry of channel assembly.

Electrophysiology. Macroscopic and single-channel current measurement follow methods in standard use in this laboratory. For these experiments, currents were recorded in the inside-out patch mode (Hamill et al., 1981). Digitization for macroscopic currents was typically at 10–50 kHz with analog filtering during acquisition (5–20 kHz, Bessel low-pass filter, −3 dB). For single-channel experiments, digitization was at 100 kHz, with 5 kHz filtering. Preparation of the pipette solution and Ca^{2+} solutions has been described previously (Wei et al., 1994; Xia et al., 1999). The pipette extracellular solution was (in mM): 140 potassium methanesulfonate, 20 KOH, 10 HEPES, and 2 $MgCl_2$, pH 7.0. Test solutions bathing the cytoplasmic face of the patch membrane contained (in mM): 140 potassium methanesulfonate, 20 KOH, 10 HEPES, pH 7.0, and one of the following: 5 mM EGTA (for nominally zero Ca^{2+} and 0.5 and 1 μM Ca^{2+} solutions), 5 mM HEDTA (for 4 and 10 μM Ca^{2+} solutions), or no added Ca^{2+} buffer (for 60, 100, and 300 μM and 1 and 5 mM Ca^{2+} solutions). The methanesulfonate solutions were calibrated against a commercial set of Ca^{2+} standards (WPI, Sarasota, FL). which yielded values essentially identical to our own Cl^--based standards. Local perfusion of membrane patches was as described previously (Solaro and Lingle, 1992; Solaro et al., 1997).

pClamp 7.0 or pClamp 8.0 for Windows (Axon Instruments, Foster City, CA) was used to generate voltage commands and to digitize currents. Current values were measured using ClampFit (Axon Instruments), converted to conductances, and then fit with a custom nonlinear least squares fitting program. Conductance–voltage (*G–V*) curves for activation were fit with a Boltzmann equation with the form:

$$G(V) = G_{max} \times (1 + \exp(-V + V_{0.5})/k)^{-1}, \quad (1)$$

where $V_{0.5}$ is the voltage of half-maximal activation of conductance, and k is the voltage dependence of the activation process (mV^{-1}). Experiments were done at room temperature (21–24°C). All salts and chemicals were obtained from Sigma (St. Louis, MO).

Simulation of G–V *curves based on partial occupancy of β2 subunit binding sites.* The strategy for evaluation of the functional consequences of channel populations containing differing stoichiometries of β:α subunits follows that outlined in previous work (Ding et al., 1998). All channels were assumed to contain four possible β subunit binding sites. Fractional occupancy by β subunits of those sites was assumed in all cases to follow a binomial distribution. At a given fractional occupancy, the fraction of channels in any of the possible stoichiometries was then calculated, and the contribution of channels of a particular stoichiometry to the overall *G–V* curves was determined based on different assumptions (e.g., independence, positive cooperativity, or negative cooperativity) about β subunit effects (Ding et al., 1998). Time constants for inactivation of a channel population containing α + β2 subunits in differing stoichiometries would be expected to exhibit up to four exponential components (corresponding to the presence of one to four inactivation domains). However, empirically, the relative amplitudes and time constants of these components result in currents that decay with a time course that can be reasonably approximated by a single exponential (Ding et al., 1998). To generate predictions for the inactivation time constant for channel populations containing some average number of β2 subunits per channel, currents were simulated and fit with single exponentials.

RESULTS

Inactivation properties of α + β2 currents indicate that channels can contain less than four inactivation domains and that inactivation domains act in an independent manner

Previous work has suggested that the inactivation properties of native inactivating BK currents among different chromaffin cells can be used as indicators of the average stoichiometry of assembly of inactivating and noninactivating subunits (Ding et al., 1998). At least in regard to inactivation behavior, each inactivating subunit appears to behave in an independent manner. Thus, the average number of inactivating subunits per channel within a population of channels defines the average inactivation rate of channels in that population. With identification of the β2 auxiliary subunit in chromaffin cells (Xia et al., 1999), this raised the possibility that variability in the average number of β2 subunits (or other inactivating β subunit) per channel may account for the previous observations in chromaffin cells.

If, in fact, inactivation properties and τ_i provide a direct assay for the stoichiometry of β2:α subunits in a channel population; it therefore becomes possible to examine the consequences of subunit stoichiometry on other channel functional properties without having specific information about the expression levels of subunits within the cell. This is particularly advantageous when it is unclear to what extent oocyte-to-oocyte variability or variability in RNA preparations may have an impact on the ability of subunits to be expressed. Using this strategy, we have therefore sought to address how channel stoichiometry may affect other functional properties of the resulting BK channels.

Specifically, the β2 subunit was coinjected with *mSlo* α subunits into *Xenopus* oocytes at different ratios, and the following aspects of BK channel function were determined: (1) the relationship between conductance and activation voltage at 10 and 300 μM Ca^{2+}; (2) the rates of onset and recovery from inactivation; (3) the ratio of inactivating to noninactivating current; and (4) the voltage dependence of steady-state inactivation.

Figure 1 shows families of currents activated by depolarizing voltage steps at either 10 or 300 μM Ca^{2+} for four different injection ratios of β2 and α subunits. Qualitatively, as the relative amount of β2 subunit is reduced, there is less current activation at potentials negative to zero, τ_i is slowed, and there is a larger noninactivating component of current at the end of the most depolarized voltage step. All of these changes are those expected for a model in which various indicators of BK channel function scale in accordance with the average number of β2 subunits per channel. This is examined more explicitly below. Another feature of the currents shown in Figure 1 is that peak current activated at positive command potentials is smaller with 300 than with 10 μM Ca^{2+}. This reflects the persistence of steady-state inactivation even after a 100 msec step to −180 mV.

The slowing of τ_i as a function of the injected ratio of β2:α subunits is illustrated in Figure 2*A* for currents obtained with 300 μM Ca^{2+} at either +100 or +160 mV. τ_i reaches a limit of ~20 msec, at ratios of both 1:1 and 2:1 suggesting that maximal occupation of α subunits by β2 subunits has occurred. The slowest observed values of τ_i are ~90 msec. This value is a bit larger than the theoretical limit of 80 msec predicted for an inactivation model involving four independent inactivation domains, in which

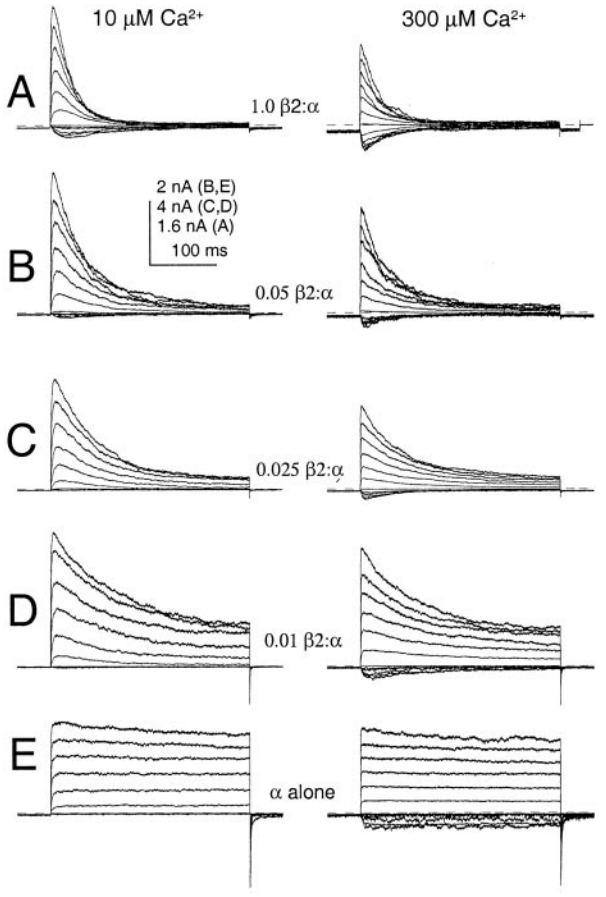

Figure 1. Decreasing the ratio of injected β2:α subunits slows the inactivation time constant of α + β2 currents. *A–E*, *Traces* show currents obtained in inside-out patches, with each patch from an oocyte injected with the indicated ratio of β2: α subunits. From *top* to *bottom*, *traces* correspond to oocytes injected with 1:1 β2:α (*A*), 0.05 β2:α (*B*), 0.025 β2:α (*C*), 0.01 β2:α (*D*), and α alone (*E*). *Left traces* were obtained in 10 μM Ca^{2+}, and *right traces* were obtained in 300 μM Ca^{2+}. *Traces* show currents activated to potentials between −100 and +120 mV in steps of 20 mV, with tail currents at −120 mV with a prepulse to −180 mV. The reduction in peak current activation with 300 μM Ca^{2+} corresponds to the additional steady-state inactivation of channels at −180 mV.

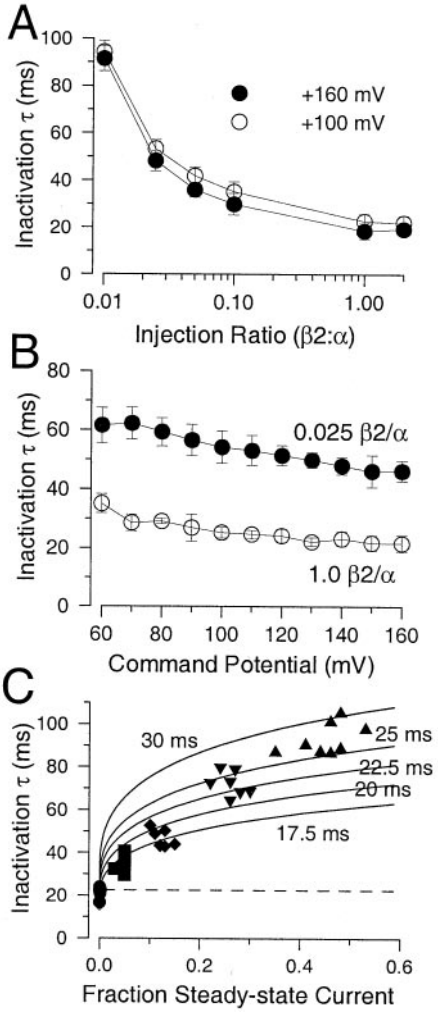

Figure 2. The inactivation properties of α + β2 currents exhibit behavior consistent with the idea that τ_i provides a direct indication of the average stoichiometry of β2:α subunits in the expressed channels. *A*, τ_i measured with 10 μM Ca^{2+} at either +160 or +100 mV is plotted as a function of the ratio of injected β2: α subunits. Each *point* is the mean of four to six patches; error bars indicate SD. *B*, τ_i is plotted as a function of command potential for 0.025 (4 patches) and 1.0 (6 patches) β2:α injection ratios. At potentials of +80 mV and more positive, the change in τ_i is small compared with the change produced by the different injection ratio. *C*, τ_i, peak current (I_p), and steady-state current (I_{ss}) were measured at various injection ratios from currents activated at +160 mV with 10 μM Ca^{2+}. f_{ss} was determined from I_{ss}/I_p and plotted as a function of the inactivation time constant observed in each patch. Each *symbol* corresponds to patches obtained from oocytes at a particular injection ratio (◇, 2.0; ●, 1.0; ■, 0.1; ◆, 0.05; ▼, 0.025; ▲, 0.01). The *curved lines* are the predictions for the relationship between τ_i and f_{ss} assuming various minimal τ_i values (as indicated, 17.5, 20, 22.5, and 25 msec), based on the model in which inactivation can be mediated by up to four independently acting inactivation domains, with one domain sufficient to produce inactivation.

20 msec is the minimal τ_i. However, measurement of the slowest τ_i values can be influenced by other factors. For example, at positive activation potentials, *Slo1* currents, even in the absence of β subunits, can exhibit a slow reduction in current during depolarization (Fig. 1*E*). The presence of such additional slow blocking components at +100 and +160 mV would tend to slow the apparent inactivation time constant resulting from β2 subunit action, which might account for the slower than expected time constants observed at the 0.01 β2:α injection ratio.

The voltage dependence of τ_i at both low (0.025) and high (1.0) ratios of β2:α subunits is plotted in Figure 2*B*. Because it is known that β subunits shift the voltage dependence of activation at a given [Ca^{2+}], a shift in τ_i might occur simply because of a shift resulting from coupling of inactivation to activation. However, over the range of +100 to +160 mV, there is little voltage dependence to τ_i at either injection ratio. This indicates that the large changes in τ_i at +160 mV that are observed as a consequence of different injection ratios must reflect the underlying stoichiometry of the inactivation process and not a consequence of a shift in activation potentials.

As mentioned in Materials and Methods, the injection ratio of β2:α subunits does not provide any handle on the stoichiometry of assembly within the oocyte. Therefore, we have attempted to use the inactivation behavior to reveal something about channel stoichiometry. As above, we measured τ_i during activation steps to +160 mV at 10 μM Ca^{2+}. For the same currents, we also measured the peak current activated by the voltage step to +160 mV and the steady-state current at the end of the voltage step (300 msec). For the simple model in which channel stoichiometries are

defined by a binomial distribution and up to four β2 subunits independently contribute to the onset of inactivation (MacKinnon et al., 1993; Ding et al., 1998), the ratio of steady-state current to peak current (f_{ss}) should vary in accordance with τ_I: at the largest steady-state current, τ_i should reach a limiting value that is approximately fourfold slower than the fastest values of τ_i. The conditions for these experiments were chosen for the following reasons. At 10 μM Ca^{2+}, there is minimal steady-state inactivation at a potential of −140 mV, so that a subsequent activation step should define the maximal current expected for the total population of expressed channels (Ding and Lingle, 2002); +160 mV was used as an activation step so that the kinetics of channel opening at 10 μM Ca^{2+} are relatively fast compared with the onset of inactivation. A drawback of the use of a step to +160 mV is that there are usually slow "inactivation" components, perhaps because of a divalent cation block that may contaminate the estimate of τ_i and steady-state current. This latter issue is most problematic for the smaller β2:α ratios.

The relationship between changes in τ_i as a function of f_{ss} is plotted in Figure 2*C* for several β2:α injection ratios. Over the range of injection ratios used, τ_i ranged from ~20 msec to time constants of >80 msec. The basic heteromultimeric model for *Shaker* K^+ inactivation (MacKinnon et al., 1993) and BK channel inactivation (Ding et al., 1998) would predict that, at the limit of the lowest ratios of β2:α subunits, τ_i should approach approximately four times that at the highest ratios. The values exhibit considerable scatter but follow the general trend required by an inactivation model in which up to four β2 subunits, each with an independently acting inactivation domain, can contribute to an intact channel containing α + β2 subunits. Lines are drawn over the data showing the predictions for this model for cases in which the minimal τ_i is 17.5–25 msec. At the lowest f_{ss}, the results appear to follow the expectations for the lines corresponding to minimal τ_i values of ~20 msec. As f_{ss} increases, values for τ_i deviate from the theoretical expectations. This was also observed in rat chromaffin cells during trypsin-mediated removal of inactivation (Ding et al., 1998). The values at high f_{ss} are likely to be in error for two reasons. The slow blocking processes mentioned above will result in slower values of τ_I, and any additional slow blocking processes will also reduce the value of f_{ss}. Both errors will contribute to the observed deviation at the lower injection ratios. However, the change in τ_i relative to f_{ss} argues strongly that channels can assemble with less than a full complement of β2 subunits and that each subunit acts in an independent manner to contribute to the onset of inactivation.

Each β2 subunit contributes incrementally to the shift in activation $V_{0.5}$

To examine the dependence of the activation of conductance on various injection ratios, *G–V* curves (for 10 μM, Fig. 3*A*; for 300 μM, Fig. 3*B*) were calculated from measurement of peak currents. As the β2:α ratio is reduced, $V_{0.5}$ at either 10 or 300 μM Ca^{2+} is shifted to more positive potentials approaching the values for α alone at the lowest β2:α ratios. For this set of patches, the full shift in *G–V* curves resulting from the β2 subunits was 77.8 mV at 10 μM and 66.3 mV at 300 μM.

There are two possible explanations for the action of β subunits that might affect the shift in *G–V* curves. In one case, as the mole fraction of β2 subunits is reduced, the fraction of channels containing less than four β2 subunits will be increased. The shift in $V_{0.5}$ could arise from channels with less than a full complement of β2 subunits having a smaller shift in $V_{0.5}$ than those with four β2 subunits. In this case, the *G–V* curves would represent a binomially weighted sum of five distinct Boltzmann functions corresponding to the five possible β2:α stoichiometries (Fig. 3*C*). Alternatively, it is possible that the shift in the *G–V* curves arises from changes in the proportion of two functional populations of channels, each with a characteristic $V_{0.5}$. Channels containing one or more β2 subunits would all share a similar $V_{0.5}$, whereas those containing no β2 subunits would appear as α alone. If so, the *G–V* curves would represent a weighted sum of two Boltzmann functions (Fig. 3*D*). This is the mechanism implied by observations in one previous study (Jones et al., 1999). This latter model might also appear to arise when there is strong cooperativity in the channel assembly process, such that channels contain either four or zero β2 subunits.

Comparison of the expectations arising from each type of model with the actual *G–V* curves obtained at 10 μM Ca^{2+} (Fig. 3A) suggests that a model in which each β2 subunit exerts some incremental contribution to the processes involved in shifting the *G–V* curve better approximates the actual results. We also considered two other cases: first, a case of strong positive cooperativity in which each additional β2 subunit associated with a channel results in a stronger effect on the $V_{0.5}$ (Fig. 3*E*); and second, a case of strong negative cooperativity in which most of the shift in $V_{0.5}$ results from the action of a single β2 subunit, with smaller effects contributed by each additional β2 subunit (Fig. 3*F*). The latter case was essentially indistinguishable from the case in which a single β2 subunit accounted for all the shift in $V_{0.5}$.

The $V_{0.5}$ for activation of conductance shifts in accordance with the fraction of injected β2 subunit (Fig. 4*A*). Similar to the relationship between τ_i and β2:α ratio, the $V_{0.5}$ reaches a limiting value at ratios of 1.0 and 2.0. Values for $V_{0.5}$ at a ratio of 0.01 approach those for *Slo1* α alone. Because there is no simple relationship between the injected ratio of β2:α subunits and the resulting channel stoichiometry, we have used the relationship between τ_i and $V_{0.5}$ to examine the effect of stoichiometry on activation $V_{0.5}$. In Figure 4*B*, the activation $V_{0.5}$ measured at 10 μM Ca^{2+} is plotted as a function of τ_i. Making a specific assumption about the minimal τ_i, τ_i can then be used to make estimates of the average number of β2 subunits per channel. *Vertical lines* correspond to the expected time constants for a channel population with an average of four, three, two, and one β2 subunits per channel. It should be realized that, except in the case of four, these expected values for the time constants are not equivalent to those predicted when all channels contain a given number of β2 subunits. This analysis suggests that the values of τ_i obtained in these experiments probably reflect average stoichiometries that vary from approximately four β2 subunits per channel to less than one β2 subunit per channel. Figure 4*B* also shows the predicted relationship between $V_{0.5}$ and τ_i expected when each β2 subunit contributes an identical amount of shift in $V_{0.5}$. The two *lines* compare predictions for the cases in which τ_{min} is 20 and 25 msec.

Given the scatter in experimental estimates and the variation in $V_{0.5}$ that seems to naturally occur among different sets of experiments, caution must be taken in attempting to relate how much shift in $V_{0.5}$ may occur in accordance with which levels of occupancy of the channels by β2 subunits. However, on the basis of the model of inactivation in which the average τ_i in a patch reflects some average, binomially distributed occupancy of channels by β2 subunits, we can calculate a predicted average number of β2 subunits per channel, relating it to the observed values for activation $V_{0.5}$ (Fig. 4*C*). The estimate of β2 subunits per channel depends on the assumption of a particular value for τ_{min}, and the

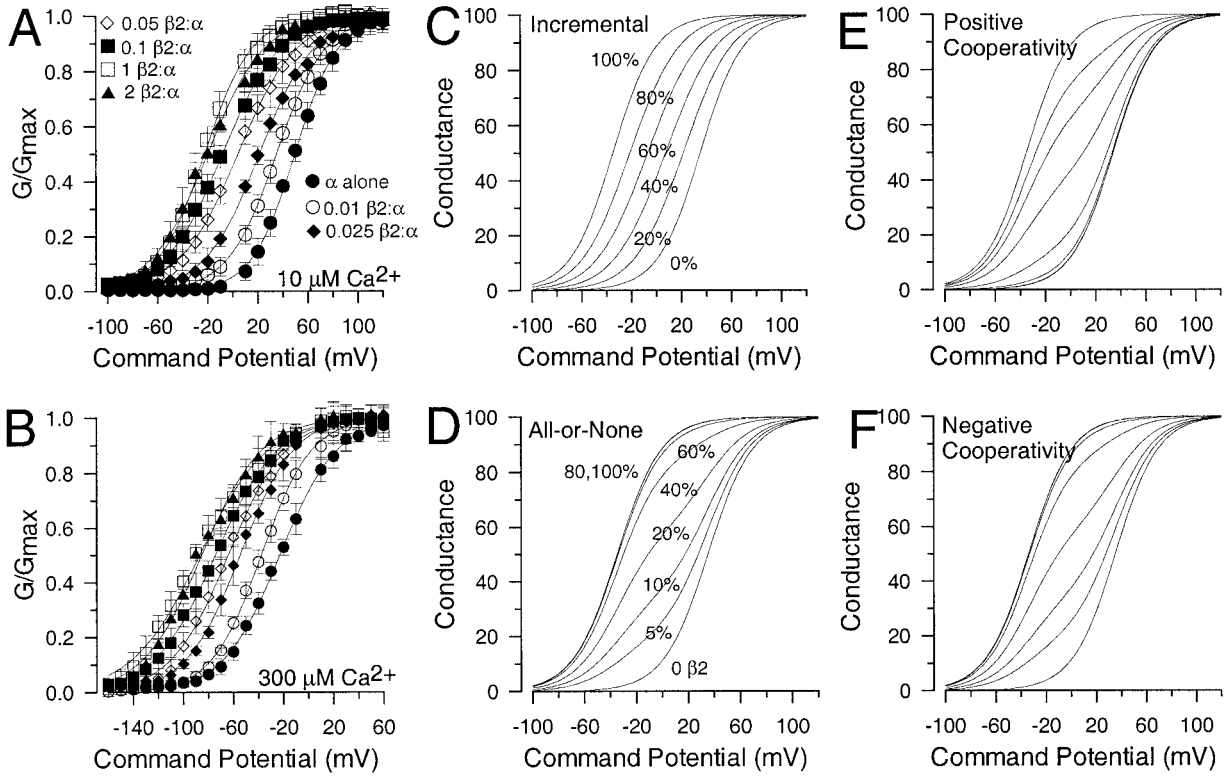

Figure 3. *G–V* curves shift in a parallel manner as a function of the injected ratio of β2 to α subunit message. Currents were generated as in Figure 1, and peak current amplitude during each activation step was used to generate *G–V* curves. Each *point* at a given injection ratio represents the mean value ± SD for a set of patches (●, α alone, 5 patches; ○, 0.01 β2:α, 4 patches; ◆, 0.025 β2:α, 4 patches; ◇, 0.05 β2:α, 5 patches; □, 0.1 β2:α, 6 patches; □, 1.0 β2:α, 5 patches; ▲, 2.0 β2:α, 4 patches). *A*, Curves were generated with 10 μM Ca^{2+}. *Solid lines* are fits of Equation 1 with values for $V_{0.5}$ of +49.6, +34.9, +21.3, +4.1, −8.2, −22.5, and −20.1 mV for β2:α ratios of 0, 0.01, 0.025, 0.05, 0.1, 1, and 2, respectively. Values of *k*, for the same ratios, were +17.3, +19.6, +21.7, +23.5, +23.0, +18.8, and +22.4 mV. *B*, Curves were generated with 300 μM Ca^{2+}. Values for $V_{0.5}$ were −23.0, −37.7, −54.3, −64.2, −74.4, −87.1, and −85.3 mV for the same injection ratios as in *A*, with values for *k* of +22.6, +19.9, +21.8, +22.9, +24.6, +27.1, and +23.6 mV. *C*, *G–V* curves were calculated for a channel population containing some average number of β2 subunits per channel, distributed binomially in the channel population. The *numbers* correspond to the percentages of the total numbers of possible sites on α subunits that are occupied by β2 subunits. The $V_{0.5}$ for activation of a channel was assumed to shift incrementally with the number of β2 subunits associated with the channel. Channels with zero β2 subunits were assumed to have a $V_{0.5}$ of +35 mV, whereas those with four β2 subunits had a $V_{0.5}$ of −35 mV; while $k = +17$ mV for all stoichiometries. Fits of Equation 1 yielded values for $V_{0.5}$ of −35, −21.2, −7.1, +7.1, +21.2, and +35 mV, with values for *k* of +17, +19.1, +20.1, +20.1, +19.1, and +17 mV. *D*, *G–V* curves were calculated as in *C*, except that the $V_{0.5}$ for a channel containing one to three β2 subunits was assumed to be identical to that of a channel containing four β2 subunits. Thus, $V_{0.5}$ was defined in an all-or-none manner by the presence of a single β2 subunit. *E*, *G–V* curves were calculated assuming positive cooperativity in the activation process from association of each additional β2 subunit with a channel. For each stoichiometry, the $V_{0.5}$ values were +35, +32.11, +26.63, +10.80, and −35 mV at average numbers of zero to four β2 subunits per channel. The increment of shift was defined from $(\text{maximal shift})^{1/4}$. *F*, *G–V* curves were calculating assuming negative cooperativity, which was indistinguishable from the case shown in *D*. As in *E*, changes in $V_{0.5}$ were defined by the one-fourth root of the full shift, except that the largest shift results from a single β2 subunit.

predicted relationship for τ_{min} values of either 20 or 25 msec is illustrated. This procedure suggests that $V_{0.5}$ appears to shift in an approximately linear manner with the number of β2 subunits per channel between the limits defined by α subunits alone and full occupancy by β2 subunits. For comparison, predictions based on models with either positive or negative cooperativity (from Fig. 3*E,F*) are also shown in Figure 4*C*, indicating that the actual results fit better with the model in which each subunit adds linearly to shift the gating equilibrium of the resulting α + β2 channels.

In sum, these results are most consistent with the view that each β2 subunit independently contributes a fixed amount to the shift in activation $V_{0.5}$.

Single α + β2 channels exist in four different channel stoichiometries, each with a different voltage dependence of activation at a given Ca^{2+}

It might be argued that the failure to observe an all-or-none effect of a single β2 subunit reflects the possibility that in macropatch recordings the *G–V* curves from two functional types of channel (Fig. 3*D*) simply average to be indistinguishable from the curves predicted for five separate functional types (Fig. 3*C*). To address this possibility, we therefore turned to single-channel recordings. In Figure 5, example sweeps and ensemble averages from single-channel patches are illustrated, corresponding to channels that inactivated with τ_i of 21.8, 33.4, 56.4, and 99 msec. A total of 49 single-channel patches were examined. A frequency histogram of the number of occurrences of single-channel inactivation time constants of various values is plotted in Figure 6*A*. Although the observed values show considerable variability, a fit of a four-component Gaussian distribution indicates that the values cluster at peaks corresponding to 22.6, 33.0, 49.1, and 99.8 msec. Although the number of examples of more slowly inactivating channels is a bit limited, these values correspond quite well to those that would be predicted for four stoichiometries with fully independent inactivation by each inactivation domain (e.g., 22, 33,

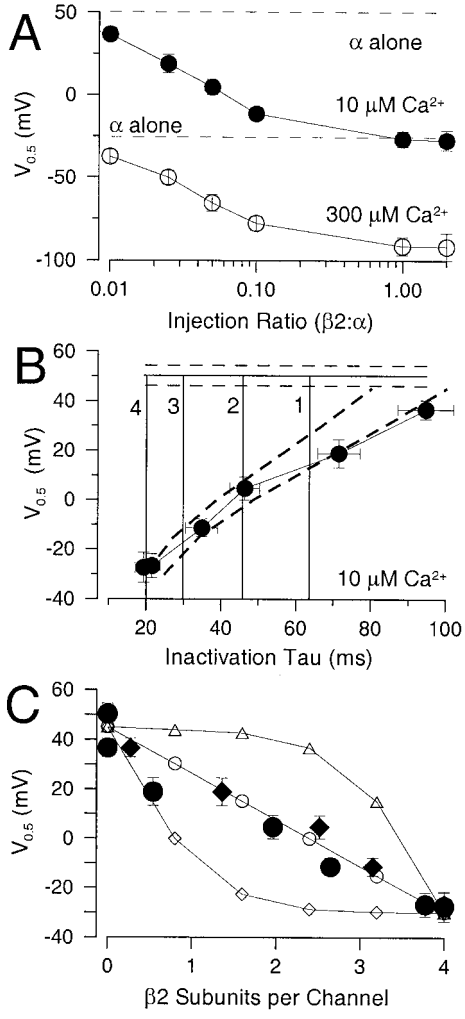

Figure 4. Dependence of $V_{0.5}$ for activation on the stoichiometry of $\alpha + \beta 2$ channels. *A*, The $V_{0.5}$ for activation is plotted as a function of $\beta 2{:}\alpha$ injection ratios for either 10 or 300 μM Ca^{2+}. Each *point* shows the mean $V_{0.5} \pm$ SD for a set of four to six patches. *B*, the mean $V_{0.5} \pm$ SD is plotted as a function of $\tau_i \pm$ SD for values measured with 10 μM Ca^{2+}. *Vertical lines 4*, *3*, *2*, and *1* correspond to τ_i expected for a binomially distributed stoichiometry with an average of four, three, two, and one $\beta 2$ subunits per channel, respectively, with the minimum τ_i assumed to be 20 msec. *Horizontal lines* correspond to $V_{0.5} \pm$ SD recorded for currents resulting from α alone. *Dashed lines* correspond to an empirical relationship between $V_{0.5}$ and τ_i for the case in which each $\beta 2$ subunit produces an incremental effect on $V_{0.5}$ as shown in Figure 3*C*. The two *lines* correspond to cases in which the minimal τ_i was assumed to be either 20 or 25 msec. *C*, *Larger symbols* plot the relationship between $V_{0.5}$ and the average number of $\beta 2$ subunits per channel calculated from the inactivation time constants. *Large* ●, Data values from *B* (obtained at 10 μM Ca^{2+}) with the assumption that the minimum τ_i for a channel with four $\beta 2$ subunits is 20 msec. ♦, Same calculation but with a minimum τ_i of 25 msec. For this conversion, when τ_i for a patch exceeded the minimal or maximal τ_i, the average number of $\beta 2$ subunits per channel was assumed to reflect either four or zero $\beta 2$ subunits, respectively. For comparison, the $V_{0.5}$ at different average numbers of $\beta 2$ subunits are shown for the cases of positive cooperativity (Fig. 3*E*; ◇) and negative cooperativity (Fig. 3*F*; △) and for an additive, incremental effect of each $\beta 2$ subunit (Fig. 3*C*; ○).

44, and 88 msec). These results provide direct evidence that individual channels can contain zero to four $\beta 2$ subunits per channel.

An interesting aspect of the single-channel recordings was that single-channel current amplitude at +100 mV appeared to scale with the number of $\beta 2$ subunits per channel, with smaller current

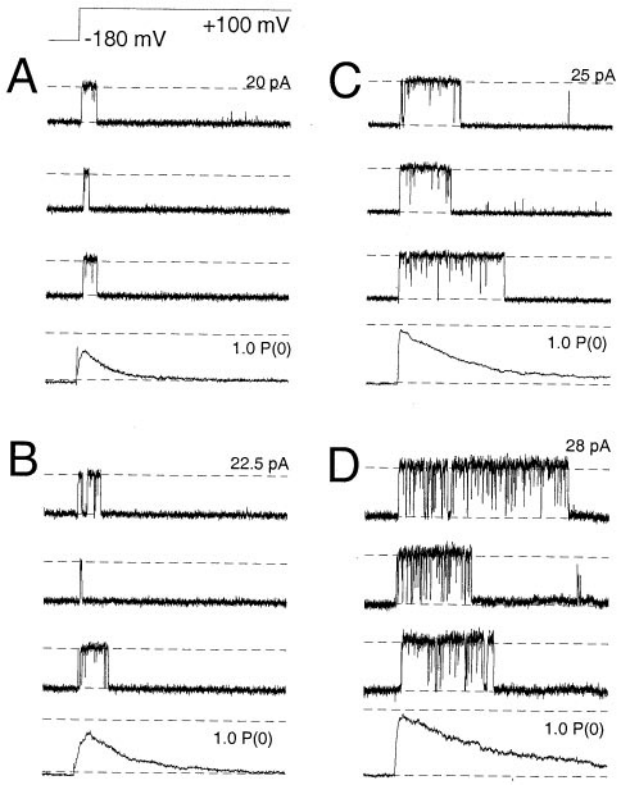

Figure 5. Single channels resulting from $\alpha + \beta 2$ coexpression reveal that individual channels can contain less than four $\beta 2$ subunits per channel. *A–D*, Traces from four different patches are illustrated. In each *panel*, the *top three traces* show records of single-channel openings, whereas the *bottom trace* shows the ensemble current average. Channel openings were activated by a voltage-step to +100 mV with 10 μM Ca^{2+}. *A*, The resulting ensemble current average exhibited a τ_i of 21.8 msec; *B*, τ_i = 33.6 msec; *C*, τ_i = 54.3 msec; *D*, τ_i = 97.9 msec. Note the differences in the single-channel current amplitude in each case measured at +100 mV. The tendency toward a larger single-channel conductance with fewer numbers of β subunits was consistently observed. There is also a tendency for channels to exhibit more frequent brief closures per unit of open time as the number of $\beta 2$ subunits per channel is reduced. For each single channel trace, the *dashed lines* indicate the open current level (*top*) and closed current level (*bottom*). For current averages, the *dashed lines* indicate P(0) levels of 1.0 (*top*) and 0.0, respectively.

amplitudes at higher numbers of $\beta 2$ subunits (Fig. 5). To confirm that observation, single-channel current measurements were made at potentials from +20 to +100 mV. Single-channel conductances were 214 ± 28.1 pS (τ_i = 21.6 ± 1.42; three patches), 228 ± 22 pS (τ_i = 31.3 ± 2.4 msec; three patches), 234 ± 14 pS (τ_i = 48.2 ± 2.5 msec; three patches), and 278 ± 15 pS (τ_i = 98.8 ± 1.2 msec; two patches), with extrapolated zero current potentials of <2 mV. The estimate under these conditions for the conductance of α alone is ~270 pS. Thus, the differences in single-channel current amplitudes seen here reflect a true difference in single-channel conductance resulting from the presence of the $\beta 2$ subunit.

We next addressed the issue of how $\beta 2{:}\alpha$ subunit stoichiometry affects activation when observed in single channels. To do this, after determination of single-channel τ_i, inactivation was then removed by brief application of trypsin (0.5 mg/ml) to the cytosolic face of patches. Ensemble averages were then generated at voltages from +20 to +140 mV using 4 μM Ca^{2+}. Four micromolar Ca^{2+} was preferable to 10 μM Ca^{2+} for this

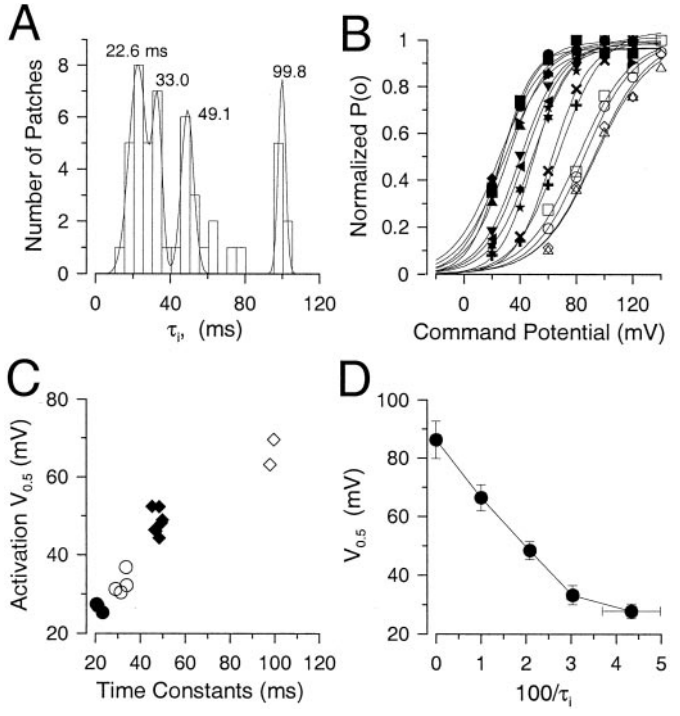

Figure 6. Channel stoichiometry revealed by inactivation correlates with an incremental shift in activation $V_{0.5}$. *A*, A frequency distribution of τ_i values determined from ensemble current averages for 49 single-channel patches is plotted. τ_i values were distributed into 5 msec bins, and a four-component Gaussian function was fit to the binned data, resulting in peak values of 22.6, 33.0, 49.1, and 99.8 msec, as indicated. For an inactivation mechanism with four independently acting inactivation domains, if channels with only one domain inactivate with a time constant of 100 msec, channels with two to four inactivation domains are predicted to inactivate with τ_i of 50, 33, and 25 msec, respectively. *B*, A set of the channels studied in *A* were briefly treated with trypsin to remove inactivation and the relationship between $P(0)$ and activation potential was determined at 4 μM Ca^{2+}. Each *filled symbol* corresponds to a different patch expressing a channel with some mixture of $\alpha + \beta 2$ subunits. *Open symbols* correspond to patches expressing α alone. *C*, The relationship between activation $V_{0.5}$ and τ_i is plotted for 15 patches studied as in *A* and *B*. Channels that exhibited a slower τ_i exhibited a more positive activation $V_{0.5}$. Values appear to cluster into four groups, which were chosen by eye and indicated by the different *symbols*. *D*, Values in *C* were grouped as indicated, and $V_{0.5}$ was plotted as a function of $100/\tau_i$; $100/\tau_i$ should reflect the number of $\beta 2$ subunits per channel assuming that a channel with one $\beta 2$ subunit inactivates with $\tau_i = 100$ msec. The value at *0* corresponds to $V_{0.5}$ values for single-channel patches containing α subunits only.

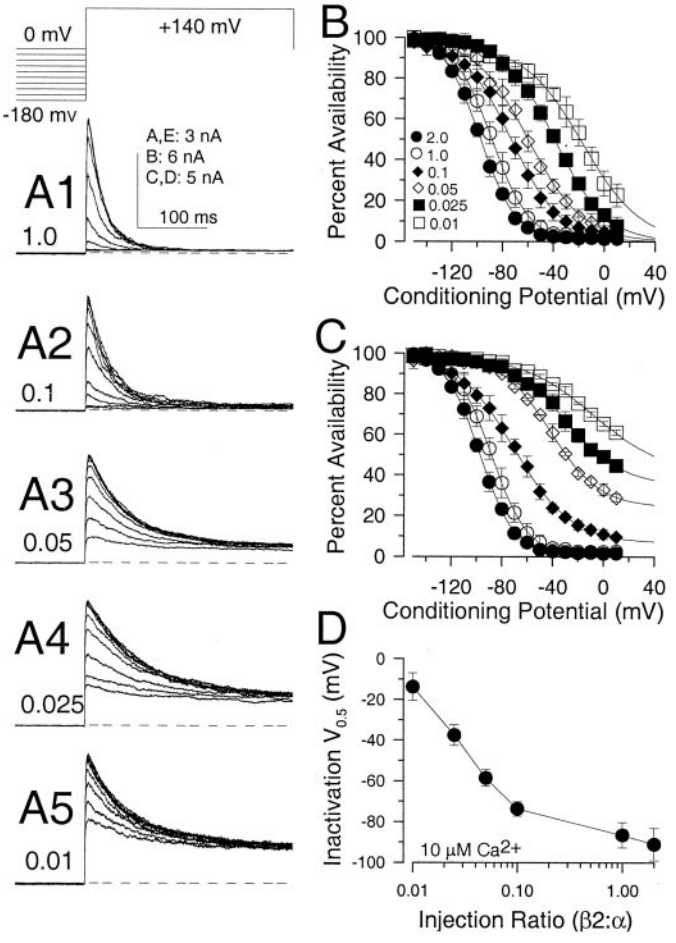

Figure 7. Steady-state inactivation shifts with changes in the $\beta 2{:}\alpha$ subunit ratio. *A1–A5*, Currents were activated with the voltage protocol indicated on the *top* for five different $\beta 2{:}\alpha$ injection ratios with 10 μM Ca^{2+}. At smaller ratios, the amount of noninactivating current increases, and the rate of inactivation slows. The duration of the conditioning step was 600 msec. The *dashed lines* indicate the 0-current level. *B*, The percent availability ± SD of only the inactivating portion of current is plotted as a function of conditioning potential for four to six patches at each of the indicated $\beta 2{:}\alpha$ injection ratios. For ratios of 0.01, 0.025, 0.05, 0.1, 1.0, and 2.0, $V_{0.5}$ values were −17.2, −38.9, −60.1, −73.1, −88.5, and −97.6 mV, respectively. *C*, The maximal current activated from different conditioning potentials was determined, providing an indication of the percent availability of the total channel population at different potentials. For ratios from 0.01 to 2.0, the voltages at which half the channels in the total population were available for activation were −97.6, −88.5, −67.8, −29.7, −3.5, and +37 mV. *D*, The voltage of half-availability determined in *B* is plotted as a function of injection ratio.

experiment, because with 4 μM Ca^{2+}, the voltage of half-activation is sufficiently positive to 0 mV both for purely $\alpha + \beta 2$ channels and for α-alone channels to allow better estimation of activation $V_{0.5}$. Figure 6*B* shows the resulting estimates of normalized open probability $P(0)$ for such trypsin-treated single-channel patches along with estimates from four patches containing α subunits alone. The $P(0)$–V curves span a range of ~60 mV, somewhat similar to that seen with macroscopic currents in Figure 3*A*. The fitted estimate of $V_{0.5}$ for each single-channel recording is plotted as a function of τ_i in Figure 6*C*. For this set of 15 single-channel patches, the values appear to cluster into four groups, with the inactivation time constant strongly correlated with the activation $V_{0.5}$. Coupled with other results presented above, this strongly argues that each $\beta 2$ subunit independently produces an equivalent effect on the resulting $V_{0.5}$ at a given $[Ca^{2+}]$.

Steady-state inactivation is also dependent on the average number of β2 subunits per channel

Other physiologically important properties of $\alpha + \beta 2$ currents may also be dependent on the stoichiometry of channel composition. Therefore, the dependence of two other properties of inactivating BK channels on the ratios of $\beta 2{:}\alpha$ subunits was also determined: first, the voltage dependence of steady-state inactivation measured at 10 μM Ca^{2+}; and second, the rate of recovery from inactivation at −140 mV also with 10 μM Ca^{2+}.

To examine steady-state inactivation properties, patches were held for at least 500 msec at conditioning potentials between −190 and +10 mV (Fig. 7*A*) before steps to +160 mV. At higher mole fractions of the $\beta 2$ subunit, steady-state inactivation mea-

sured with 10 μM cytosolic Ca^{2+} was essentially identical to that previously observed for inactivating BK channels in RIN cells (Li et al., 1999), and for BK_i channels in chromaffin cells (Ding and Lingle, 2002). The fractional availability of current as a function of the initial conditioning potential was determined. As the ratio of β2:α was reduced, the fractional availability of the resulting BK current was shifted to more positive potentials, and at the lowest dilutions it is clear that there is a substantial amount of current that does not inactivate. Because the activation step was to +160 mV, any channel that contains even one inactivation domain will contribute little to the steady-state current. Thus, the steady-state current represents almost exclusively the fraction of channels that contain no β2 subunits. The currents were analyzed in two ways. First, we measured only the fractional availability of the inactivating portion of the current (Fig. 7*B*). This takes into account only those channels that contain at least one β2 subunit. We also plotted the total amount of current available from any conditioning potential (Fig. 7*C*). This provides a better indication of the entire channel population at each β2:α dilution. Qualitatively, it is quite clear that reducing the ratio of injected β2:α subunits results in two effects: first, a marked shift in the fractional availability of channels for activation; and second, an increase in the fraction of channels that do not inactivate. The dependence of the voltage of half-channel availability on injection ratio is shown in Figure 7*D*.

Recovery from inactivation exhibits an anomalous dependence on β2:α ratio

The time constant of recovery from inactivation (τ_r) was defined at 10 μM with a paired pulse protocol in which, after complete inactivation of the channels at +140 mV, a second test step to +140 mV followed a variable recovery interval at −140 mV (Fig. 8*A*). At high β2:α ratios, τ_r was ~20–25 msec similar to values measured for inactivating BK channels in RIN cells (Ding et al., 1998; Li et al., 1999). As the ratio of β2:α was reduced (Fig. 8*B,C*), τ_r became faster, appearing to reach a limiting value at ~5 msec at the smallest ratios of β2:α.

This change of τ_r with the ratio of β2:α would appear to contradict previous work in which progressive trypsin-mediated removal of inactivation of inactivating BK channels in chromaffin cells did not alter τ_r (Ding et al., 1998). For a model of a block in which occupancy of a blocking site by a single inactivation domain is sufficient to produce inactivation, if recovery is governed solely by dissociation of a single domain from its blocking site, no alteration in τ_r is expected as the number of inactivation domains per channel is altered. Thus, the present result would seem to conflict with previous results and may challenge one simple conception of the molecular steps involved in the inactivation process, namely that the recovery process should be governed by dissociation by a single inactivation domain from its blocking site.

Is there a possible explanation for the dependence of recovery from inactivation on channel stoichiometry that would not require us to discard the view that dissociation of a single inactivation determines recovery? One simple explanation of this result is that it does not reflect some unusual aspect of the inactivation mechanism per se but rather reflects the coupling of recovery from inactivation to Ca^{2+}-dependent activation steps. In fact, for both BK_i currents in chromaffin cells and α + β2 currents, the time course of recovery from inactivation becomes faster both at more negative potentials and with reductions in cytosolic Ca^{2+} (Ding and Lingle, 2002). Thus, although dissociation of a single inactivation particle may be sufficient to remove inactivation, it

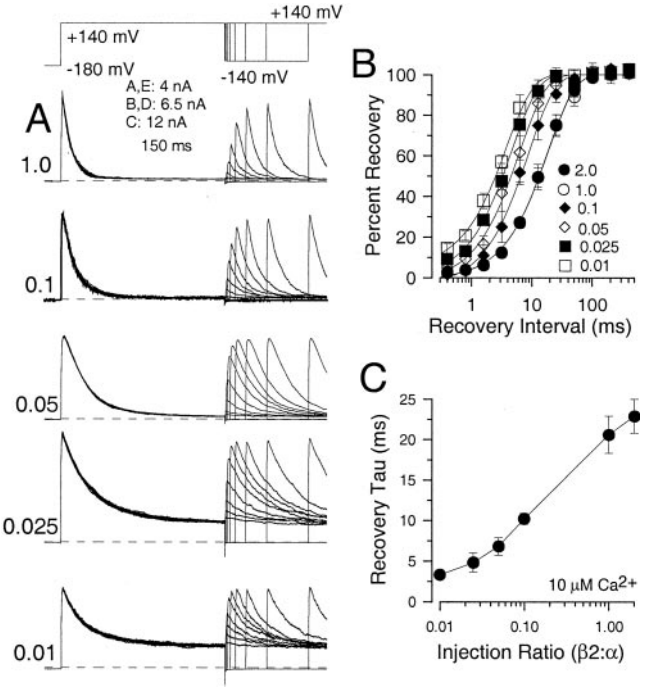

Figure 8. Recovery from inactivation shifts with changes in the β2:α subunit ratio. *A*, Currents were activated with 10 μM with the paired pulse recovery protocol shown on the *top*. Each set of *traces* corresponds to a different β2:α injection ratio as indicated. Note the much slower recovery from inactivation at 1.0 β2:α than at lower ratios. The *dashed lines* indicate the 0-current level. *B*, The percent recovery ± SD is displayed as a function of recovery interval for a set of four to six patches at each injection ratio. The recovery time points at a ratio of 1.0 are obscured by those at 2.0. The recovery time course was fit in each case with a single exponential. For ratios of 0.01, 0.25, 0.05, 0.1, 1.0, and 2.0, τ_r was 3.9, 4.8, 6.5, 9.0, 19.3, and 19.0 msec, respectively. *C*, The dependence of τ_r on the injection ratio is displayed.

seems likely that, dependent on Ca^{2+} and recovery potential, channels may reinactivate during the recovery process. As a consequence, the time course of recovery from inactivation most likely reflects multiple kinetic steps, including dissociation of an inactivation domain, but also other Ca^{2+}-dependent transitions. Because reductions in the β2:α injection ratio shift the $V_{0.5}$ for activation to more positive values, this would naturally then be expected to also produce effects on recovery from inactivation.

Two sets of experiments were done to test this idea. First, we examined the time course of recovery from inactivation after different amounts of removal of inactivation of α + β2 currents by trypsin. Similar to our previous results (Ding et al., 1998; Li et al., 1999), when the average number of inactivation domains per channel is altered by digestion with trypsin, the time course of recovery from inactivation remains virtually unchanged (results not shown). The difference between the experiment with trypsin and the results with β2:α dilution is that, in the former case, channels with fewer inactivation domains still have a full set of β subunits per channel, thereby leaving the voltage dependence of activation unchanged. In a second type of experiment, the average number of inactivation domains per channel was altered not by dilution of β2 subunits but by coexpression of β2 and α subunits, along with a β2 subunit in which the N-terminal inactivation domain has been removed (construct β2-Δ33; Xia et al., 1999). Thus, a full complement of β2 subunits will be available to associate with α subunits, but less than a full complement of inactivation domains will be present. We varied the ratio of

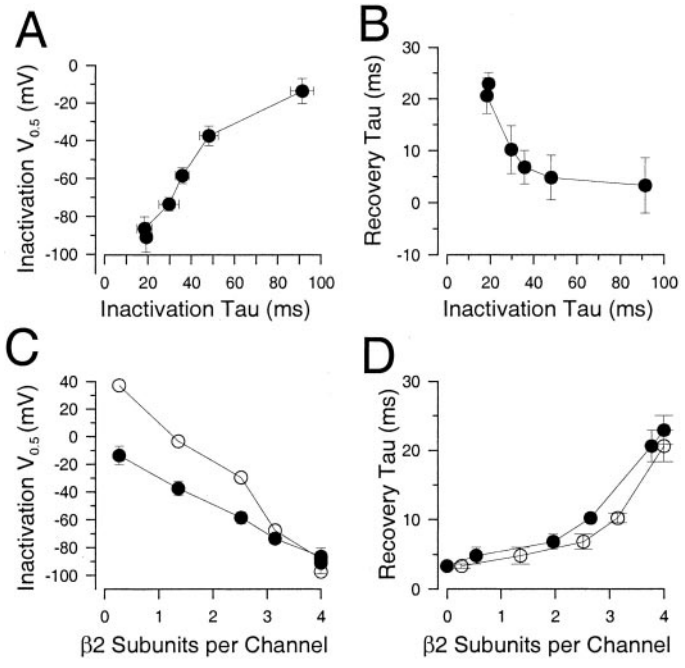

Figure 9. Dependence of steady-state inactivation and recovery from inactivation on β2:α stoichiometry in α + β2 channels. *A*, Inactivation $V_{0.5}$ determined exclusively for the inactivating portion of current is plotted as a function of the inactivation time constant for the same set of patches. *B*, τ_r is plotted as a function of the inactivation time constant. *C*, Inactivation $V_{0.5}$ determined either from the inactivating portion of the current (●) or from the whole channel population (○) is related to the average number of β2 subunits per channel based on the inactivation properties of the currents. The inactivating portion of the current appears to vary with subunit stoichiometry in a manner qualitatively similar and parallel to the activation $V_{0.5}$ (Fig. 4). *D*, τ_r is plotted as a function of subunit stoichiometry and exhibits a surprisingly steep dependence on the apparent number of β2 subunits per channel. Other experiments described in Results indicate that this does not reflect some complexity in the stoichiometry of the unblocking portion of the inactivation process but rather reflects the coupling of recovery to shifts in the voltage dependence of activation.

β2:β2-Δ33 to change the number of inactivation domains per channel in the population. Regardless of the ratio of β2:β2-Δ33, the time course of recovery is indistinguishable whether channels inactivate with time constants of 20–30 or 60–70 msec.

The above results therefore support the view that the seemingly anomalous faster rate of recovery from inactivation with smaller β2:α ratios is simply a consequence of the influence of current activation transitions on the recovery time course (Ding and Lingle, 2002). In essence, τ_r is not dependent on the number of inactivation domains per channel but rather on the number of β subunits per channel because of coupling of the recovery process to steps in the activation pathway. An interesting implication of this result is that variation in τ_r based on the stoichiometry of β2:α subunit assembly suggests a novel mechanism by which key functional properties of BK_i current might be regulated.

To summarize how steady-state inactivation and τ_r vary in accordance with the stoichiometry of those channels, we have plotted $V_{0.5}$ for steady-state inactivation and τ_r as a function of τ_i (Fig. 9*A,B*). To evaluate the extent to which stoichiometry may affect the inactivation $V_{0.5}$ and τ_r, these parameters were also plotted (Fig. 9*C,D*) against the predicted average number of β2 subunits per channel based on the analysis of τ_i presented in Figure 4. Because both the inactivation $V_{0.5}$ and τ_r are complex functions of both inactivation and activation transitions, mechanistic interpretation of the correspondence of these parameters with β2 subunit stoichiometry is substantially more complicated. Thus, we present these figures primarily for their physiological significance, i.e., that alteration of β2:α subunit stoichiometry can affect key functional properties of the resulting α + β2 currents that are likely to influence the role such channels can play among different cells.

Each β1 subunit also produces an incremental effect on shifts in $V_{0.5}$ at a given Ca^{2+}

Previous work suggested that a single β1 subunit in association with four α subunits might be sufficient to produce a full shift in the $V_{0.5}$ for activation (Jones et al., 1999). Therefore, a few experiments were done to test whether the observations described above were unique to the β2 subunit. Currents resulting from activation of α + β1 channels were studied after injection of different ratios of β1:α subunit (Fig. 10*A*). These currents resulted in *G–V* curves that exhibited a relatively parallel shift (Fig. 10*B*) more similar to the predictions of the incremental model for β subunit action than an all-or-none model. We also examined *G–V* curves at injection ratios likely to result in intermediate stoichiometries (e.g., 0.1 β1:α) at different days after injection to try to identify conditions that might mimic previous results (Jones et al., 1999). In no case have we observed *G–V* curves that exhibit the clear separation into distinct Boltzmann components that was observed previously (Jones et al., 1999).

To verify that a range of stoichiometric combinations of β1 and α subunits were occurring, we also examined the activation characteristics of β1 channels in which the N terminus from the β2 subunit was appended (construct β1–C2). Coexpression of α + β1–C2 subunits resulted in inactivating currents similar to wild-type α + β2 currents (Fig. 10*C*), although the limiting τ_i appeared a bit slower. If the assembly of α + β1 subunits was such that only 0:4 and 4:4 combinations were occurring, the currents at each injected ratio should simply show two components, an inactivating component always with the same τ_i and a sustained component that increases as the fraction of β1 subunit is reduced. This is not observed, indicating that a range of stoichiometric combinations of β1–C2 and α subunits are occurring. The *G–V* curves for activation of α + β1–C2 currents shifted the β1–C2:α subunit ratio in an approximately parallel manner (Fig. 10*D*).

We therefore evaluated the relationship between τ_i, f_{ss}, and $V_{0.5}$ for activation for the α + β1–C2 currents. As shown in Figure 11*A*, τ_i varies with f_{ss} in a manner consistent with an inactivation mechanism similar to that for the α + β2 currents. In this case, the α + β1–C2 currents are best approximated by a model in which the limiting minimal τ_i is ~30 msec. In Figure 11*B*, the activation $V_{0.5}$ is plotted as a function of τ_i for both the β1–C2 construct and β2. The relationships are similar, although the $V_{0.5}$ for activation at 10 μM Ca^{2+} is shifted to somewhat more negative potentials for the β1–C2 construct. Consistent with this, the full range of shift in $V_{0.5}$ produced by the β1–C2 construct relative to α alone was closer to −100 mV rather than the near −80 mV observed for the β2 construct. On the basis of the analysis described above, the values of τ_i obtained for the β1–C2 construct were then related to the predicted average number of β subunits per channels assuming a τ_{min} of 30 msec and a τ_{max} of 120 msec. Over a broad range of predicted channel stoichiometries, $V_{0.5}$ varies approximately linearly with the predicted number of β subunits per channel (Fig. 11*C*). This is the result consistent with an incremental effect of each β1 subunit on $V_{0.5}$

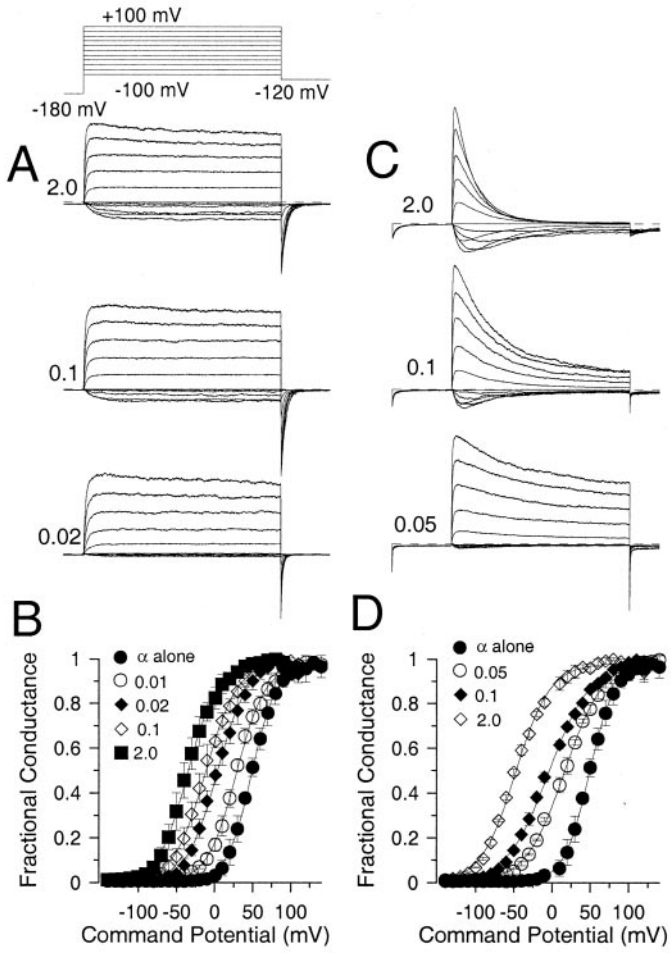

Figure 10. Dilution of the β1:α ratio causes partial shifts in activation $V_{0.5}$. *A*, α + β1 currents were activated with 10 μM Ca^{2+} with the indicated voltage protocol at β1:α injection ratios of 2.0, 0.1, and 0.02. *B*, *G–V* curves were generated for sets of four to six patches for α alone and four different β1:α injection ratios. Over all dilutions, the curves exhibit essentially parallel changes with some reduction in the slope at the intermediate dilutions. For ratios of 0, 0.01, 0.02, 0.1, and 2.0, $V_{0.5}$ values were +48.9, +28.8, +4.1, −11.4, and −34.9 mV, respectively. *C*, α subunits were coexpressed with a β1 construct with the β2 N terminus appended upstream of the first transmembrane segment (termed β1–C2). Currents were activated with 10 μM Ca^{2+} with the voltage protocol shown in *A*. The presence of inactivation in this construct provides an independent measure of the stoichiometry of assembly. *D*, *G–V* curves were generated for a set of patches from traces similar to those shown in *C*. Activation $V_{0.5}$ values were +48.9, +17.0, −3.7, and −47.8 mV for ratios of 0, 0.05, 0.1, and 2.0, respectively.

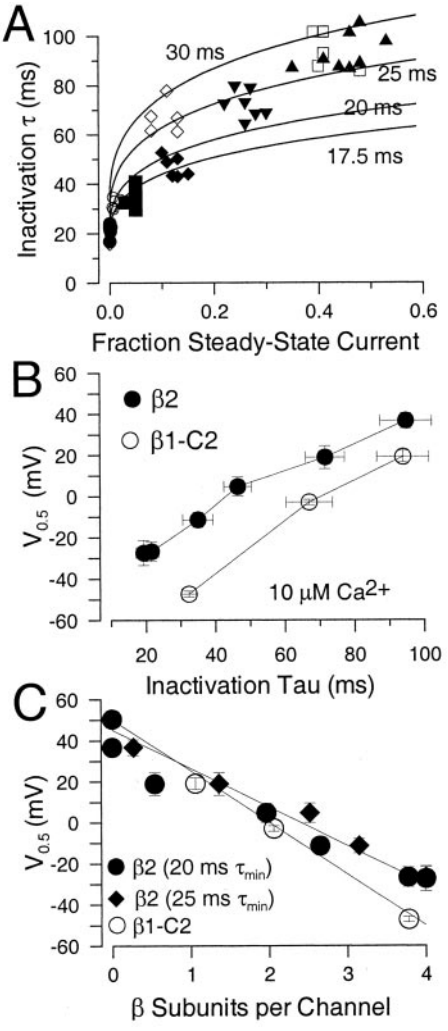

Figure 11. Shifts in activation $V_{0.5}$ resulting from changes in the β1:α ratio reflect an incremental effect of each individual β1 subunit on activation gating. *A*, the variation of τ_i with f_{ss} is displayed for both α + β2 currents (*solid symbols* as in Fig. 2*C*) and for α + β1–C2 currents [β1–C2:α injection ratios of 2 (*open circles*), 0.1 (*open diamonds*), and 0.05 (*open squares*)]. For the α + β1–C2 currents, the variation in τ_i is consistent with the idea that each inactivation domain acts independently to produce inactivation, with one subunit being sufficient to produce inactivation. *B*, The relationship between activation $V_{0.5}$ and τ_i is plotted for β2 and β1–C2. Both exhibit a similar behavior with perhaps somewhat different minimal τ_i values at the highest β:α ratios. *C*, τ_i was related to the average number of β subunits per channel following a procedure used in Figure 4. τ_{min} used to relate τ_i to the channel stoichiometry was 30 msec for the β1–C2 construct. The β1 subunit was assumed to produce a somewhat larger voltage shift (−90 mV) than that produced by the β2 subunit (−70 mV). The linearity in the relationship between activation $V_{0.5}$ and the number of β subunits per channel supports the view that each individual β subunit contributes incrementally to the shifts in activation gating.

and is inconsistent with the all-or-none effect of a single β1 subunit.

DISCUSSION

The pore-forming core of virtually all ion channels consists of a multimeric structure, arising either from assembly of identical or related subunits or from repeated elements contained with the same protein. In addition, many ion channels, including representatives of both voltage- and transmitter-gated families, exist as complexes in which one or more kinds of auxiliary subunits coassemble with the pore-forming α subunits. In the case of BK channels, the auxiliary β subunit KCNMB family appears to play a critical role in defining almost every important functional property of the channel complex, including the apparent Ca^{2+} dependence of gating (McManus et al., 1995; Meera et al., 1996; Wallner et al., 1999; Xia et al., 1999), activation and deactivation behavior (Brenner et al., 2000), inactivation (Wallner et al., 1999; Xia et al., 1999, 2000; Uebele et al., 2000), and even instantaneous current–voltage behavior (Zeng et al., 2001). Because the stoichiometry of assembly of α and β subunits is 1:1 (Knaus et al., 1994a), the tetrameric BK channels can contain up to four β subunits.

Here we have taken advantage of the properties of inactivation conferred by β2 auxiliary subunits to examine the consequences

of different stoichiometric combinations of $\alpha + \beta 2$ subunits on functional properties of the channels. We first establish that the inactivation properties of macroscopic $\alpha + \beta 2$ currents resulting from different $\beta 2{:}\alpha$ ratios are generally consistent with the idea that functional channels are formed with less than a full complement of $\beta 2$ subunits. This is also directly supported by single-channel recordings. Using inactivation as an indicator of the average number of $\beta 2$ subunits per channel, we then relate other channel functional properties to the channel stoichiometry. The analysis of both macroscopic and single-channel currents argues that each $\beta 2$ subunit contributes incrementally to influence the activation $V_{0.5}$ at a given Ca^{2+} concentration. A similar conclusion was obtained with the $\beta 1$ subunit. In addition to activation $V_{0.5}$, both the $V_{0.5}$ for steady-state inactivation and the time constant of recovery from inactivation varied with channel stoichiometry. The pronounced effect of $\beta 2{:}\alpha$ stoichiometry on inactivation $V_{0.5}$ and τ_r supports the view that variation in BK channel properties in cells can be continuously varied by the ratio of β to α subunits.

Dependence of gating behavior on $\beta{:}\alpha$ stoichiometry

Compared with channels containing only α subunits, the $\beta 2$ subunit shares with the $\beta 1$ subunit an ability to shift the equilibrium between closed and open states to more negative voltages at a given $[Ca^{2+}]$. The present results suggest that association of each $\beta 2$ subunit independently exerts an incremental effect on the gating equilibrium. On the basis of inactivation time constants, we were able to make inferences about the average number of $\beta 2$ subunits per channel at a given injection ratio. Examination of the amount of shift in the $V_{0.5}$ with fractional occupancy by $\beta 2$ subunits suggests that the $V_{0.5}$ shifts in a relatively linear manner with the fractional occupancy of $\beta 2$ subunit sites. In contrast, models in which the effect of each additional $\beta 2$ subunit exhibits either positive or negative cooperativity predict curvature in the relationship between $V_{0.5}$ and the average number of $\beta 2$ subunits per channel. Thus, the $V_{0.5}$ for activation shifts with changes in occupancy of the α subunit by the $\beta 2$ subunits in a manner consistent with each β subunit contributing a fixed change in the free energy difference between closed and open states at a given $[Ca^{2+}]$. Thus, there is neither positive nor negative cooperativity among $\beta 2$ subunits in regard to shifting the $V_{0.5}$ for activation.

Several studies have examined how the $\beta 1$ subunit influences gating behavior (Nimigean and Magleby, 1999, 2000; Cox and Aldrich, 2000), although these studies allow no predictions about the impact of $\beta{:}\alpha$ subunit stoichiometry. On the basis of one gating model, it has been suggested that $\beta 1$ subunits influence a number of aspects of gating, including effects on the Ca^{2+} affinity of both closed and open states, the equilibrium of the closed to open transition, and the equilibrium of voltage sensor movement (Cox and Aldrich, 2000). Similarly, single-channel analysis (Nimigean and Magleby, 1999, 2000) reveals effects of the $\beta 1$ subunit on both channel burst durations and opening frequency. Thus, β subunits appear to influence multiple aspects of BK gating. A question that must now be addressed is how the incremental change in $V_{0.5}$ observed for each β subunit may be reconciled with current gating models.

Comparison with previous studies

Several other studies also support the idea that BK channels in native cells may exist in stoichiometries reflecting five functional categories of channels. Our analysis of BK_i currents in chromaffin cells suggested that such currents arise from the tetrameric assembly of inactivating and noninactivating subunits (Ding et al., 1998). However, how this assembly might relate to activation $V_{0.5}$ was not addressed. In human coronary smooth muscle, BK channels were observed to exhibit five different $P(0)$ versus V curves, incrementally spanning over 120 mV (Tanaka et al., 1997), presumably reflecting five populations of possible $\beta 1{:}\alpha$ subunit assemblies. Similarly, BK channels from the avian nasal salt gland, when studied in lipid bilayers, also clustered into five different apparent Ca^{2+} sensitivities (Wu et al., 1996), which were interpreted to reflect the five stoichiometric combinations of two subunits, one of higher and one of lower Ca^{2+} affinity.

These previous studies contrast with the conclusions of one other study in which it was suggested that the contribution of a single $\beta 1$ subunit to a channel was sufficient to produce an all-or-none effect on the shift in gating (Jones et al., 1999). The main points in favor of the all-or-none model were the following. As the ratio of $\beta 1{:}\alpha$ increased, the shift in activation $V_{0.5}$ for macroscopic currents exhibited a very steep change from α- to $\alpha + \beta 1$-like. For those patches with a $V_{0.5}$ intermediate between the two extremes, the *G–V* curves exhibited two-component Boltzmann relationships similar to the predictions of the all-or-none model (Fig. 3*D*). Furthermore, when kinetic properties of single channels in patches from oocytes injected with low $\beta 1{:}\alpha$ ratios were examined, individual channels exhibited either of two different open interval behaviors, one comparable with *Slo1* channels alone and one with a longer open time. We consider these results quite convincing that channels with a behavior intermediate between that with α alone and that with $4\beta 1{:}4\alpha$ were not observed, although we know of no simple way to reconcile these previous results with our own.

The present results have the advantage that the inactivation properties provide an independent indication that channels with intermediate stoichiometries do actually occur. Thus, one possibility is that the conditions of expression in the Jones study somehow resulted in channels with either 0:4 or 4:4 $\beta 1{:}\alpha$ stoichiometries, although it is difficult to imagine how this might occur. One difference between the study of Jones et al. (1999) and our own is that the molar $\beta{:}\alpha$ ratios used here appear substantially higher than those used in the other study. Another difference was the use of 4:26 and 3:31 α subunit splice variants (Jones et al., 1999) in contrast to the 0:3 variant used here.

Although these explanations remain unsatisfying, for the present we propose that, when a direct measure of subunit stoichiometry is available, each β subunit produces an incremental effect on channel gating. However, under some as yet undefined conditions, $\beta{:}\alpha$ subunit assembly is sufficiently highly cooperative that the resulting channel population can contain primarily 0:4 and 4:4 $\beta{:}\alpha$ combinations, thereby resulting in the functional equivalent of an all-or-none β subunit effect.

β subunits and the functional diversity of BK channel properties

BK channels in native tissues exhibit great diversity in their functional properties (McManus, 1991; Vergara et al., 1998), and, most notably, different BK channels exhibit substantial variation in their activation ranges at a given $[Ca^{2+}]$. This reflects an important contribution of different β subunits to the BK channel complex among different tissues, with some lesser contribution of different α subunit splice variants.

Variation in the average stoichiometry of $\beta{:}\alpha$ subunits among cells clearly can play a key role in defining the gating properties of the BK channels. Such a mechanism has been proposed to ac-

count for the role of BK channels in frequency tuning in hair cells (Jones et al., 1998, 1999). The present results provide additional support for the idea that the activation range for a population of BK channels can be continuously adjusted on the basis of the fractional occupancy of the each α subunit with an appropriate β subunit. Furthermore, for inactivating BK channels, both channel availability and the rate of return from inactivation also vary continuously as a function of the average β:α subunit stoichiometry within the channel population. Thus, these results indicate that essentially every physiologically important parameter of BK channel function can be substantially regulated by adjustment of the relative expression of β to α subunits.

REFERENCES

Adelman JP, Shen KZ, Kavanaugh MP, Warren RA, Wu YN, Lagrutta A, Bond CT, North RA (1992) Calcium-activated potassium channels expressed from cloned complementary DNAs. Neuron 9:209–216.

Brenner R, Jegla TJ, Wickenden A, Liu Y, Aldrich RW (2000) Cloning and functional characterization of novel large conductance calcium-activated potassium channel β subunits, hKCNMB3 and hKCNMB4. J Biol Chem 275:6453–6461.

Butler A, Tsunoda S, McCobb DP, Wei A, Salkoff L (1993) mSlo, a complex mouse gene encoding "maxi" calcium-activated potassium channels. Science 261:221–224.

Cox D, Aldrich R (2000) Role of the β1 subunit in large-conductance Ca^{2+}-activated K^+ channel gating energetics. Mechanisms of enhanced Ca^{2+} sensitivity. J Gen Physiol 116:411–432.

Ding J, Lingle C (2002) Steady-state and closed-state inactivation properties of inactivating BK channels. Biophys J, in press.

Ding JP, Li ZW, Lingle CJ (1998) Inactivating BK channels in rat chromaffin cells may arise from heteromultimeric assembly of distinct inactivation-competent and noninactivating subunits. Biophys J 74:268–289.

Hamill OP, Marty A, Neher E, Sakmann B, Sigworth FJ (1981) Improved patch-clamp techniques for high-resolution current recording from cells and cell-free membrane patches. Pflugers Arch 391:85–100.

Jones EM, Laus C, Fettiplace R (1998) Identification of Ca^{2+}-activated K^+ channel splice variants and their distribution in the turtle cochlea. Proc R Soc Lond B Biol Sci 265:685–692.

Jones EM, Gray-Keller M, Fettiplace R (1999) The role of Ca^{2+}-activated K^+ channel spliced variants in the tonotopic organization of the turtle cochlea. J Physiol (Lond) 518:653–665.

Knaus HG, Garcia-Calvo M, Kaczorowski GJ, Garcia ML (1994a) Subunit composition of the high conductance calcium-activated potassium channel from smooth muscle, a representative of the mSlo and slowpoke family of potassium channels. J Biol Chem 269:3921–3924.

Knaus HG, Folander K, Garcia-Calvo M, Garcia ML, Kaczorowski GJ, Smith M, Swanson R (1994b) Primary sequence and immunological characterization of beta-subunit of high conductance Ca^{2+}-activated K^+ channel from smooth muscle. J Biol Chem 269:17274–17278.

Li ZW, Ding JP, Kalyanaraman V, Lingle CJ (1999) RINm5f cells express inactivating BK channels whereas HIT cells express noninactivating BK channels. J Neurophysiol 81:611–624.

MacKinnon R, Aldrich RW, Lee AW (1993) Functional stoichiometry of Shaker potassium channel inactivation. Science 262:757–759.

McManus OB (1991) Calcium-activated potassium channels: regulation by calcium. J Bioenerg Biomembr 23:537–560.

McManus OB, Helms LM, Pallanck L, Ganetzky B, Swanson R, Leonard RJ (1995) Functional role of the beta subunit of high conductance calcium-activated potassium channels. Neuron 14:645–650.

Meera P, Wallner M, Jiang Z, Toro L (1996) A calcium switch for the functional coupling between alpha (hslo) and beta subunits (Kv,cabeta) of maxi K channels. FEBS Lett 385:127–128.

Meera P, Wallner M, Toro L (2000) A neuronal beta subunit (KCNMB4) makes the large conductance, voltage- and Ca^{2+}-activated K^+ channel resistant to charybdotoxin and iberiotoxin. Proc Natl Acad Sci USA 97:5562–5567.

Nimigean CM, Magleby KL (1999) The beta subunit increases the Ca^{2+} sensitivity of large conductance Ca^{2+}-activated potassium channels by retaining the gating in the bursting states. J Gen Physiol 113:425–440.

Nimigean CM, Magleby KL (2000) Functional coupling of the beta(1) subunit to the large conductance Ca^{2+}-activated K^+ channel in the absence of Ca^{2+}. Increased Ca^{2+} sensitivity from a Ca^{2+}-independent mechanism. J Gen Physiol 115:719–736.

Solaro CR, Lingle CJ (1992) Trypsin-sensitive, rapid inactivation of a calcium-activated potassium channel. Science 257:1694–1698.

Solaro CR, Ding JP, Li ZW, Lingle CJ (1997) The cytosolic inactivation domains of BK_i channels in rat chromaffin cells do not behave like simple, open-channel blockers. Biophys J 73:819–830.

Tanaka Y, Meera P, Song M, Knaus HG, Toro L (1997) Molecular constituents of maxi KCa channels in human coronary smooth muscle: predominant alpha + beta subunit complexes. J Physiol (Lond) 502:545–557.

Uebele VN, Lagrutta A, Wade T, Figueroa DJ, Liu Y, McKenna E, Austin CP, Bennett PB, Swanson R (2000) Cloning and functional expression of two families of beta-subunits of the large conductance calcium-activated K^+ channel. J Biol Chem 275:23211–23218.

Vergara C, Latorre R, Marrion NV, Adelman JP (1998) Calcium-activated potassium channels. Curr Opin Neurobiol 8:321–329.

Wallner M, Meera P, Ottolia M, Kaczorowski GJ, Latorre R, Garcia ML, Stefani E, Toro L (1995) Characterization of and modulation by a beta-subunit of a human maxi KCa channel cloned from myometrium. Receptors Channels 3:185–199.

Wallner M, Meera P, Toro L (1999) Molecular basis of fast inactivation in voltage and Ca^{2+}-activated K^+ channels: a transmembrane beta-subunit homolog. Proc Natl Acad Sci USA 96:4137–4142.

Wei A, Solaro C, Lingle C, Salkoff L (1994) Calcium sensitivity of BK-type KCa channels determined by a separable domain. Neuron 13:671–681.

Weiger TM, Holmqvist MH, Levitan IB, Clark FT, Sprague S, Huang WJ, Ge P, Wang C, Lawson D, Jurman ME, Glucksmann MA, Silos-Santiago I, DiStefano PS, Curtis R (2000) A novel nervous system beta subunit that downregulates human large conductance calcium-dependent potassium channels. J Neurosci 20:3563–3570.

Wu JV, Shuttleworth TJ, Stampe P (1996) Clustered distribution of calcium sensitivities: an indication of hetero-tetrameric gating components in Ca^{2+}-activated K^+ channels reconstituted from avian nasal gland cells. J Membr Biol 154:275–282.

Xia XM, Ding JP, Lingle CJ (1999) Molecular basis for the inactivation of Ca^{2+}- and voltage-dependent BK channels in adrenal chromaffin cells and rat insulinoma tumor cells. J Neurosci 19:5255–5264.

Xia X-M, Ding J, Zeng X-H, Duan K-L, Lingle C (2000) Rectification and rapid activation at low Ca^{2+} of Ca^{2+}-activated, voltage-dependent BK currents: consequences of rapid inactivation by a novel β subunit. J Neurosci 20:4890–4903.

Zeng X-H, Xia X-M, Lingle CJ (2001) Gating properties conferred on BK channels by the β3b auxiliary subunit in the absence of its N- and C-termini. J Gen Physiol 117:607–627.